PLANETARY SCIENCE

Potassium isotope anomalies in meteorites inherited from the protosolar molecular cloud

Y. Ku* and S. B. Jacobsen

Potassium (K) and other moderately volatile elements are depleted in many solar system bodies relative to CI chondrites, which closely match the composition of the Sun. These depletions and associated isotopic fractionations were initially believed to result from thermal processing in the protoplanetary disk, but so far, no correlation between the K depletion and its isotopic composition has been found. Our new high-precision K isotope data correlate with other neutron-rich nuclides (e.g., ^{64}Ni and ^{54}Cr) and suggest that the observed ^{41}K variations have a nucleosynthetic origin. We propose that K isotope anomalies are inherited from an isotopically heterogeneous protosolar molecular cloud, and were preserved in bulk primitive meteorites. Thus, the heterogeneous distribution of both refractory and moderately volatile elements in chondritic meteorites points to a limited radial mixing in the protoplanetary disk.

INTRODUCTION

Thermal processing in the solar nebula is believed to have depleted solar system bodies in moderately volatile elements (MVEs) (*1*) and fractionated their isotopes by partial condensation of the nebular gas (*2*, *3*) and/or evaporation during planetesimal collisions (*4*). Among the moderately volatile and relatively abundant elements, only potassium (K) has more than one stable isotope (^{39}K and ^{41}K), with ^{41}K being primarily the decay product of the short-lived ^{41}Ca [$t_{1/2}$ ~ 0.1 million years (Ma) (*5*)]. These characteristics make K a good candidate for studying the history of nucleosynthetic components and thermal processing in the early solar system.

Many planetary bodies show variable depletions in K, often quantified by the K/U ratio. One advantage of this ratio is that it can be measured remotely by a γ-ray survey (*6*). For chondritic and planetary samples, Ca/K is a better indicator of K depletions because Ca is one of the refractory major elements, with well-defined and relatively constant concentrations in different solar system bodies. Early work on K isotopes in solar system bodies found no differences within an uncertainty of ~0.5‰ (*2*). Recent higher-precision (~ 0.1‰) K isotope data show K isotopic fractionation of ~0.4‰ between the Earth and the Moon (*7*), interpreted as a result of incomplete vapor condensation during Moon formation. More recently, observed K isotope variations among planetary bodies and chondrites (*8*–*11*) were interpreted to result from potential K loss from their parent bodies. If the thermal processing (evaporation/condensation) that depleted K has also fractionated K isotopes, a correlation between K isotopic compositions and K depletions is expected. However, no clear correlation has been found so far. Apparently, the processes that depleted K in the solar system bodies did not fractionate K isotopes to an observable degree.

Stellar nucleosynthetic processes (e.g., p-, s-, and r-processes) can also result in K isotope variations, because ^{41}Ca, the source of most ^{41}K, is mainly produced by an s-process (*12*). These variations are likely preserved in chondritic meteorites because they are thought to have accreted in the accretionary disk from materials that formed in the solar nebula and/or were inherited from the presolar molecular cloud. Small isotopic anomalies have been found in chondrites for many neutron-rich isotopes (*13*–*17*). While the causes of these anomalies remain uncertain, an incomplete mixing of materials from different stellar sources is a leading explanation. If the observed ^{41}K variations are of nucleosynthetic origin, correlations between ^{41}K and other neutron-rich nuclides in chondrites are expected.

To constrain the astrophysical environment and understand the thermal events that occurred a few million years before and after the formation of the solar system, we carried out high-precision [~30 parts per million (ppm); fig. S2A] K isotope measurements of samples from a number of solar system objects. We studied both chondrites of different petrologic types and samples of differentiated planetary bodies, aiming to evaluate the contributions of stellar nucleosynthetic processes and mass-dependent fractionations to the observed ^{41}K variations. K isotopic compositions were measured using the multicollector inductively coupled plasma mass spectrometry (ICP-MS) Nu Sapphire and are expressed relative to our laboratory standard, Merck Suprapur: $\delta^{41}K\ (‰) = (((^{41}K/^{39}K)_{sample}/(^{41}K/^{39}K)_{standard} - 1) \times 10^3$. Uncertainties are reported at the two-sigma level (2SE). For a convenient conversion, other commonly used standards were also measured relative to Suprapur: Seawater and NIST SRM-3141a yielded $\delta^{41}K = +0.215 \pm 0.024‰$ and $+0.047 \pm 0.003‰$, respectively (fig. S5 and table S1). The $\delta^{41}K$ notation and K isotopic standards are described in detail in section S1.

RESULTS

We found well-resolved $\delta^{41}K$ differences among different planetary bodies, including Mars, Earth, and Vesta, as well as between ordinary (O), enstatite (E), and carbonaceous (C) chondrites (Fig. 1 and Table 1). The samples of the same chondritic meteorites from different sources yield similar $\delta^{41}K$ values, suggesting the homogeneity of the samples and robustness of the measurements.

The Orgueil $\delta^{41}K$ value

Two individual pieces of CI chondrite analyzed in this work, Orgueil-2 and Orgueil-3, were obtained from different sources to establish the $\delta^{41}K$ value of CI meteorites, which are considered the best representation of the starting material in the solar system. The mean $\delta^{41}K$ value of −0.133‰ for the CI group is calculated on the basis of these two samples. The original $\delta^{41}K$ value for CI chondrites that was

Department of Earth and Planetary Sciences, Harvard University, 20 Oxford Street, Cambridge, MA 02138, USA.
*Corresponding author. Email: yku@g.harvard.edu

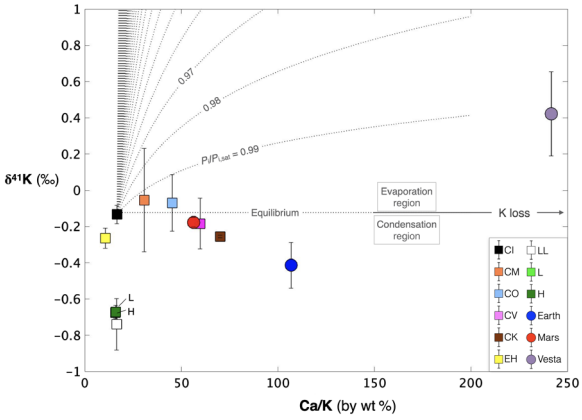

Fig. 1. Chemical and isotopic variations of K among chondrites and planetary bodies. Each data point is the group mean calculated using available samples within each group. The corresponding uncertainties on the group means are larger than the analytical uncertainty because of the heterogeneity among different meteorites within groups (details in Table 1). Note that evaporation/condensation cannot explain our K isotopic data. The K and Ca concentrations in each group are taken from the literature (*32*, *45*–*47*). The group mean and uncertainties (2SE) for the CI group in this study are based on Orgueil.

published in (*7*) and that has been widely used in the literature [e.g., (*11*)] is indistinguishable from the bulk silicate earth (*18*). In this study, we analyzed the same material from (*7*) and found that this sample contains nearly 8 weight % (wt %) Earth crustal materials, based on major and trace element compositions. This implies that most of its K is terrestrial, not meteoritic. This issue is discussed in detail in section S2 and in figs. S3 and S4.

The δ^{41}K of chondrites

The group mean δ^{41}K and the corresponding 2SE are calculated on the basis of different meteorites (described in Materials and Methods). The mean δ^{41}K value is −0.054‰ for CM chondrites, −0.070‰ for CO chondrites, −0.184‰ for CV chondrites, −0.255‰ for one CK chondrite, −0.264‰ for EH chondrites, and −0.696‰ for the main cluster of the ordinary chondrites (H, L, and LL). The ordinary chondrites have the lightest δ^{41}K among all samples analyzed. The H and L chondrite δ^{41}K values form a single cluster in the δ^{41}K-Ca/K ratio diagram (Fig. 1), but one LL chondrite, Parnallee, has a substantially lighter δ^{41}K value of −0.917‰ (Table 1). We have analyzed interior materials (Holbrook-1) and the fusion crust [Holbrook-1(c)] of the same meteorite and found indistinguishable δ^{41}K values. There are small variations of δ^{41}K in carbonaceous chondrites, but the mean δ^{41}K value (CM, CO, and CV) is indistinguishable from CI chondrites. Enstatite chondrites (EH), which are enriched in K, have a lighter δ^{41}K value relative to CI chondrites. The mean of EL chondrites is not included because the two samples analyzed have very different δ^{41}K values (Table 1 and section S1).

The δ^{41}K of achondrites

The samples of differentiated planetary bodies show differences in K isotopic compositions, with the mean δ^{41}K values being −0.177‰ for Mars and +0.422‰ for the eucrite parent body, which generally agree with (*9*). Mars might have a unique bulk composition in the inner solar system, intermediate between carbonaceous chondrites and Earth. The eucrite parent body, Vesta, is strongly volatile-depleted and shows an enrichment in ^{41}K compared to other meteorites and Earth. The bulk mean Earth, which is depleted in K relative to both carbonaceous and ordinary chondrites, has an intermediate δ^{41}K value of −0.414‰. The mean value is determined on the basis of three samples—BCR-2, BHVO-2, and CHEPR (mid-ocean ridge basalt)—to be consistent with the previous work (*18*).

Our results are generally consistent with previously published δ^{41}K values after correcting for different standards (fig. S5), except for one CI δ^{41}K derived from a contaminated sample (*7*, *11*). Some inconsistencies and larger δ^{41}K variations observed in previous studies (*8*, *11*) are likely due to the use of nonrepresentative samples (~0.1 g), and the substantial use of meteorite finds. Samples studied here, on the other hand, were mostly meteorite falls powdered from more than 2 g of whole rock (up to 200 g). In addition, many meteorites were obtained from multiple sources to overcome the possible heterogeneity of individual pieces. Despite a general agreement in the mean δ^{41}K values for each meteorite group between this study and (*11*), we favor discussion and interpretation of the data based on samples studied here (see section S3).

DISCUSSION

Mass-dependent fractionation of K isotopes during evaporation/condensation

Variations in δ^{41}K are often explained by evaporation/condensation processes, which could occur under kinetic or equilibrium conditions. In the case of equilibrium ($P_i/P_{i,sat} = 1$, where $P_{i,sat}$ is the saturation pressure for species i), the isotopic composition of the condensed phase must be heavier than the bulk system, but the magnitude of fractionation (the horizontal dotted line in Fig. 1) is expected to be smaller than the current analytical uncertainty. Under $P_i/P_{i,sat} < 1$, evaporation of K from a condensed phase would enrich the residue in ^{41}K. The magnitude of fractionation increases from a near-equilibrium value to 22‰ (*19*) as the $P_i/P_{i,sat}$ ratio decreases to ~0 (Fig. 1 and section S4). If $P_i/P_{i,sat} > 1$, the condensate is expected to be depleted in ^{41}K, with the magnitude of fractionation decreasing to ~0‰ as condensation continues in a closed system. Thus, if CI chondrites were the starting material for the solar nebula, then the observed magnitude of K isotopic fractionation in K-depleted samples cannot be explained by the loss of K during evaporation or condensation. Therefore, single-stage nebular thermal processing cannot account for the observed nebula-wide δ^{41}K variations.

While other MVEs such as Zn and Cu (*20*) also show depletion in planetary bodies, K behaves very differently from them. For example, Zn and Cu are more easily fractionated during impact vaporization (*21*–*23*), but no K isotopic fractionation was found in tektites (*24*). A lack of correlations between δ^{41}K and δ^{66}Zn and δ^{65}Cu (fig. S6) (*11*) further suggests incoherent behaviors among MVEs during nebula thermal processes and planetary formation (*25*). We have also considered parent body processes (i.e., aqueous alteration) and conclude that these processes cannot explain the overall K isotope variations in chondrites. A constant K-Rb ratio has been found for different meteorite groups studied here and the bulk Earth (fig. S7). In addition, we found that δ^{41}K versus Al/K, Cr/K, Fe/K, and Ni/K in different chondrite groups and Earth show the same pattern, regardless of whether the element that K is compared to is mobile or immobile (fig. S7). The observed δ^{41}K variations could be due to a heterogeneous distribution of either anomalous presolar grains or local aqueous alteration products. We have minimized

Table 1. K isotopic composition of each sample in this study. The interior portion and fusion crust of Holbrook-1 were powdered independently; the fusion crust, Holbrook-1 (c), is not included in calculating the group mean. NIST SRM-3141-a was measured with respect to Suprapur = +0.047 ± 0.003‰. The group mean and the corresponding 2SE are calculated on the basis of different meteorites. Details are in Materials and Methods. *N*, numbers of independent analytical runs; *n*, total number of the bracketed δ^{41}K values from *N* days; ANSMET, Antarctica Meteorite Collection (NASA); ASU, Center for Meteorite Studies, Arizona State University; Caltech (JW), Caltech Jerry Wasserburg; HMNH, Harvard Museum of Natural History; Harvard (CL), Harvard University (Charlie Langmuir); MNHN, Museum national d'Histoire naturelle; NEMS, New England Meteoritical Services; SAO (JW), Smithsonian Astrophysical Observatory (John Wood); SAO (UM), Smithsonian Astrophysical Observatory (Ursula Marvin); USNM3529, Smithsonian USNM3529, 4-kg Allende powder.

Group	Sample	Find/Fall	Type	δ^{41}K Suprapur (‰)	±2SE*	*N*	*n*	Group mean	±2SE	Crushed powder (g)	Sources	δ^{41}K SRM-3141a (‰)
CI	Orgueil-2a	Fall	CI1	−0.125	0.030	5	21			0.11	SAO (JW)	−0.172
	Orgueil-2b			−0.192	0.030	5	26					−0.239
	Orgueil-3	Fall	CI1	−0.107	0.038	3	14	−0.133†	0.051	1024	MNHN	−0.154
CM	Murray-1a	Fall	CM2	0.205	0.033	4	19			0.29	SAO (JW)	0.158
	Murray-1b			0.241	0.046	2	9					0.194
	Mighei-1a	Fall	CM2	−0.255	0.046	2	10			1.94	SAO (JW)	−0.302
	Mighei-1b			−0.246	0.046	2	9					−0.293
	Murchison-1a	Fall	CM2	−0.112	0.030	10	50			10.00	SAO (UM)	−0.159
	Murchison-1b			−0.155	0.065	1	5	−0.054	0.285			−0.202
CO	Ornans-1	Fall	CO3.4	−0.012	0.029	5	24			0.88	SAO (JW)	−0.059
	Ornans-2	Fall	CO3.4	−0.057	0.038	3	14			6.45	MNHN	−0.104
	DaG 749	Find	CO3	−0.216	0.038	3	17			1.75	ASU	−0.263
	NWA7916	Find	CO3	0.136	0.033	4	21			1.60	ASU	0.089
	Kainsaz	Fall	CO3.2	−0.165	0.038	3	14	−0.070	0.157	1.70	NEMS	−0.212
CV	Allende-1a	Fall	CV3	−0.187	0.030	10	50			34	SAO (UM)	−0.234
	Allende-1b			−0.197	0.030	9	46					−0.244
	Allende-2	Fall	CV3	−0.035	0.033	4	19			4000	USNM3529	−0.082
	Vigarano-1a	Fall	CV3	−0.237	0.033	4	19			0.67	SAO (JW)	−0.284
	Vigarano-1b			−0.270	0.046	2	9	−0.184	0.140			−0.317
CK	NWA6254	Find	CK4	−0.255	0.046	2	12			2.22	ASU	−0.302
EH	Abee-1a	Fall	EH4	−0.293	0.025	7	36			1.00	NEMS	−0.340
	Abee-1b			−0.292	0.046	2	9					−0.339
	Indarch-1a	Fall	EH4	−0.119	0.038	3	15			1.82	NEMS	−0.166
	Indarch-1b			−0.160	0.033	4	22					−0.207
	Indarch-2	Fall	EH4	−0.333	0.038	3	15	−0.264	0.056	0.23	HMNH	−0.380
EL	MacHill 88481	Find	EL3	−0.556	0.038	3	15			0.44	ANSMET	−0.603
	Eagle	Fall	EL6	0.082	0.046	2	9			0.69	NEMS	0.035
LL	Tuxuac-1a	Fall	LL5	−0.609	0.046	2	11			2.46	NEMS	−0.656
	Tuxuac-1b			−0.543	0.038	3	14					−0.590
	Parnallee	Fall	LL3	−0.917	0.038	3	17			1.34	ASU	−0.964
	Vicencia	Fall	LL3	−0.759	0.038	3	17			1.32	ASU	−0.806
	Chainpur	Fall	LL3.4	−0.708	0.046	2	10	−0.740	0.141	0.99	SAO (JW)	−0.755
L	Marion Iowa	Fall	L6	−0.679	0.030	5	22			2.00	HMNH	−0.726
	Homestead	Fall	L5	−0.725	0.030	6	29			2.00	HMNH	−0.772
	Bruderheim	Fall	L6	−0.672	0.038	3	15			70	SAO (UM)	−0.719
	Peace River-1	Fall	L6	−0.632	0.038	3	15			190	SAO (UM)	−0.679

continued on next page

Group	Sample	Find/Fall	Type	δ^{41}K Suprapur (‰)	±2SE*	*N*	*n*	Group mean	±2SE	Crushed powder (g)	Sources	δ^{41}K SRM-3141a (‰)
	Peace River-2	Fall	L6	−0.672	0.033	4	22			0.12	Caltech (JW)	−0.719
	Holbrook-1	Fall	L6	−0.636	0.038	3	25			0.93	SAO (JW)	−0.683
	Holbrook-1 (c)	Fall		−0.621	0.038	3	25			0.60		−0.668
	Holbrook-2	Fall	L6	−0.658	0.046	2	10	−0.675	0.028	3.07	HMNH	−0.705
H	Kernouve	Fall	H6	−0.628	0.030	5	23			2.00	HMNH	−0.675
	Dresden	Fall	H6	−0.681	0.030	5	24			2.00	HMNH	−0.728
	Forest City	Fall	H5	−0.724	0.030	6	27			2.00	HMNH	−0.771
	Grady	Find	H3	−0.710	0.038	3	15			70	Caltech (JW)	−0.757
	Guareña	Fall	H6	−0.681	0.038	3	15			53.40	Caltech (JW)	−0.728
	Estacado	Find	H6	−0.609	0.038	3	15	−0.672	0.037	2.80	NEMS	−0.656
Mars	Nakhla-1	Fall	Nakhla	−0.193	0.029	5	27			0.25	SAO (JW)	−0.240
	Nakhla-2	Fall	Nakhla	−0.164	0.029	5	25			0.23	SAO (JW)	−0.211
	QUE94201.55	Find	Shergottite	−0.152	0.038	3	15			0.10	ANSMET	−0.199
	Zagami-1	Fall	Shergottite	−0.279	0.038	3	15			0.11	NEMS	−0.326
	Zagami-2	Fall	Shergottite	−0.120	0.038	3	14	−0.177	0.027	0.94	ASU	−0.167
Vesta	Stannern	Fall	Eucrite	0.503	0.038	3	9			0.26	SAO (JW)	0.456
	Bouvante	Find	Eucrite	0.270	0.038	3	12			0.13	SAO (JW)	0.223
	Sioux County	Fall	Eucrite	0.202	0.038	3	16			0.20	SAO (JW)	0.155
	Juvinas	Fall	Eucrite	0.712	0.046	2	10	0.422	0.232	0.14	SAO (JW)	0.665
Earth	BHVO-2		Basalt	−0.333	0.030	9	46				USGS	−0.380
	BCR-2		Basalt	−0.370	0.030	9	46				USGS	−0.417
	CHEPR		Basalt	−0.538	0.033	4	18	−0.414	0.126		Harvard (CL)	−0.585
				Internal uncertainty = 30 ppm								

*The uncertainty (2SE) is 2SD (65 ppm)/$\sqrt{N}$ (fig. S2) and was replaced with 30 ppm if less than 30 ppm. Additional uncertainty is negligible when converting Suprapur to SRM-3141a. †The meteorite group means and 2SE are based on small numbers (numbers of different meteorites); CI group is based on two chunks of one meteorite, Orgueil.

these effects by using large samples (up to 200 g) whenever possible and using group means for each meteorite class based on multiple samples. Thus, we argue that the mean δ^{41}K of each group should minimize these effects of small-scale sample heterogeneity.

Evidence supporting the type II supernova injection

Alternatively, the observed variations of δ^{41}K in meteorites may reflect a heterogeneous distribution of ^{41}Ca in the solar nebula. The presence of extinct ^{41}Ca (now ^{41}K) found in Ca-Al–rich inclusions (CAIs) (*26*) could result from either in situ irradiation, through the ^{42}Ca(p, pn)^{41}Ca reaction, or injection by a recent supernova explosion. Thus, the observed ^{41}K variations could potentially reflect varying proportions of Ca-rich (CAIs) and Ca-poor (chondrules and matrix) components of chondrites. Using available literature data and mass-balance calculations, we found that the contribution of ^{41}K from CAIs to the total ^{41}K balance is not sufficient to explain the observed K isotope variations in meteorites (details can be found in section S6).

Therefore, ^{41}K (decay product of ^{41}Ca) must have been heterogeneously distributed in the protosolar molecular cloud; such heterogeneity was preserved in the solar nebula and recorded in the primitive meteorites. The inhomogeneous distribution of ^{41}K could be caused by one or more injections of ^{41}K from a nearby stellar source into the presolar molecular cloud. ^{41}Ca is primarily formed via neutron capture from abundant and stable ^{40}Ca and may be continuously ejected from massive stars during their Wolf-Rayet phase or ejected by final explosions of supernovae (*27*, *28*). The main sources of presolar ^{41}K (^{41}Ca) are still debated, but it is almost certain that when a massive star explodes in a supernova, neutron-rich isotopes are ejected into the molecular cloud, which become part of the solar nebula materials (*29*, *30*). Neutron capture extinct radionuclides (e.g., ^{41}Ca, ^{129}I) and neutron-rich isotopes, especially the ones in the Fe peak (e.g., ^{48}Ca, ^{50}Ti, ^{54}Cr, and ^{64}Ni), are likely formed by nuclear reactions in stars shortly before the solar system formation (*31*). Because most ^{41}Ca has decayed to ^{41}K due to its half-life of ~0.1 Ma, massive stellar winds and supernova ejecta would add abundant ^{41}K and little ^{41}Ca to the solar nebula materials.

To evaluate whether K isotopic variations could result from an injection of ^{41}K, we compare δ^{41}K to ε^{64}Ni and ε^{54}Cr (Fig. 2). The mass-independent anomalies in ^{64}Ni and ^{54}Cr (expressed in ε-notation)

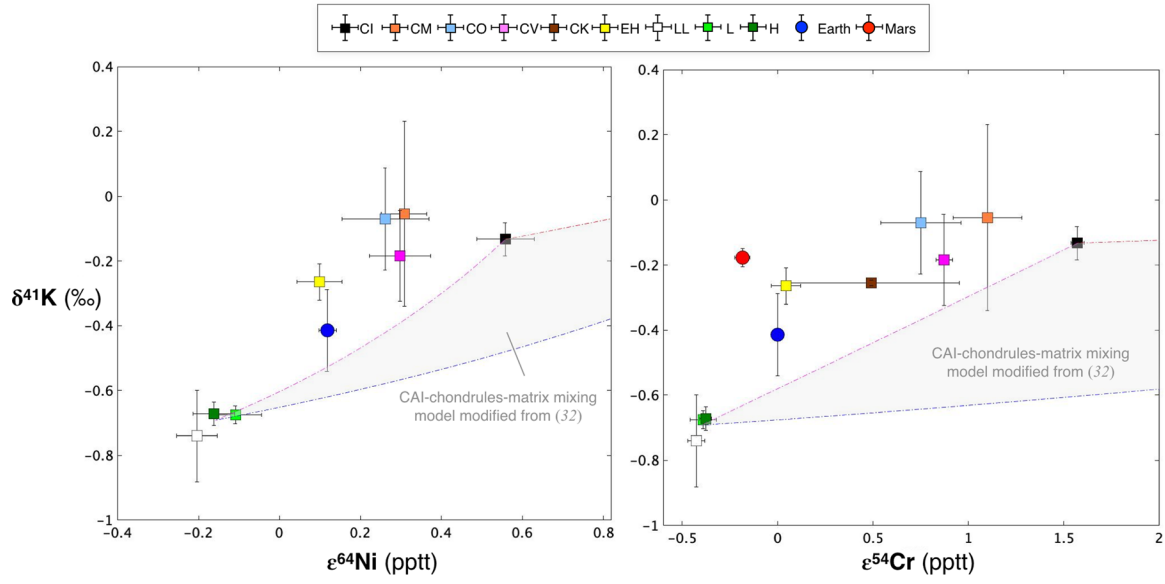

Fig. 2. Variations of $\delta^{41}K$, $\varepsilon^{54}Cr$, and $\varepsilon^{64}Ni$ in bulk samples. The concentrations of each element are from (*32*, *45*), and mean $\varepsilon^{54}Cr$ and $\varepsilon^{64}Ni$ data for each group are from (*17*) (see fig. S8 for complete references). The gray regions show the three-component mixing model [modified from (*32*)] of chondrules, matrix, and CAIs. The chondrule and matrix components are estimated by the average ordinary and CI chondrites, respectively. The correlations between $\delta^{41}K$, $\varepsilon^{54}Cr$, and $\varepsilon^{64}Ni$ suggest that these anomalies are primarily caused by nucleosynthetic processes and cannot be generated by a multicomponent mixing model between major chondrite components. The correlations also cannot be explained by the mixing of two isotopically distinct reservoirs, such as CM (or CI) and ordinary chondrites. This is because mixing between two end members would yield straight lines in $\delta^{41}K$-Ca/K plots (Fig. 1, and similar plots in fig. S7B), which is not observed. In addition, mixing the two end members' compositions is unlikely to reproduce both volatile-depleted Earth and volatile-enriched enstatite chondrites that both have intermediate values of $\delta^{41}K$, $\varepsilon^{64}Ni$, and $\varepsilon^{54}Cr$. pptt, parts per ten thousand.

are generally thought to reflect the heterogeneous distribution of distinct nucleosynthetic components in the solar system (*13*–*15*). We found positive correlations between ^{41}K, ^{64}Ni, and ^{54}Cr, suggesting that ^{41}Ca (the precursor of ^{41}K) was probably produced in a type II supernova shell (*15*). This implies that the observed K isotopic variations reflect the heterogeneous distribution of presolar nuclides in the solar system. Earth, which is usually an end member in many nucleosynthetic isotope anomaly plots, such as $\mu^{142}Nd^*$ and $\varepsilon^{92}Mo$ (fig. S9), has an intermediate value between the carbonaceous and ordinary chondrites in $\delta^{41}K$, $\varepsilon^{64}Ni$, and $\varepsilon^{54}Cr$. The varying sequence of objects in each diagram (Fig. 2 and fig. S9) suggests that the correlations of $\delta^{41}K$ with other isotopes cannot simply be due to a mixing between two end members, CM (or CI) and ordinary chondrites. Instead, possibly more than two nucleosynthetic components were present to explain the overall solar system anomalies observed in neutron-rich isotopes.

Testing a multicomponent mixing model

The chemical and isotopic compositions of chondrites result from mixing several components formed under different physicochemical conditions. For example, Alexander (*32*) used a four-component mixing model to successfully reproduce the K concentrations in six carbonaceous chondrite groups. These components are as follows: (i) CAIs, (ii) matrix of the CI composition, (iii) chondrules compositionally similar to the volatile-depleted CI chondrites, and (iv) H_2O-rich ices. Bloom *et al.* (*11*) used a similar model to explain the $\delta^{41}K$ variations observed in carbonaceous chondrites by the mixing of chondrules and matrix. The matrix $\delta^{41}K$ was approximated by the bulk CI $\delta^{41}K$ value of −0.53‰, while the chondrule $\delta^{41}K$ value ranging from −0.28 to 2.08‰ was calculated assuming fractional evaporative K loss (1 to 10%) from initial CI composition described by the Rayleigh fractionation law. However, because the initial CI $\delta^{41}K$ value of −0.53‰ measured in the contaminated Orgueil sample is incorrect, both modeled $\delta^{41}K$ values are also incorrect. Once the wrong initial CI $\delta^{41}K$ value of −0.53‰ is replaced with the correct one of −0.133‰, the mixing model fails to account for the observed $\delta^{41}K$ variations in both carbonaceous and ordinary chondrites. Thus, mixing of different components that experienced various degrees of thermal processing in the solar nebula is an unlikely explanation for the overall K isotope variations found in chondrites.

Let us now evaluate whether the four-component mixing model of (*32*) can reproduce the observed $\delta^{41}K$- $\varepsilon^{64}Ni$ and $\delta^{41}K$-$\varepsilon^{54}Cr$ correlations. Because ices are supposed to contain no K, Ni, and Cr, such a model reduces to three components with unknown $\delta^{41}K$ values. Following (*32*), we approximate matrix with the bulk CI $\delta^{41}K$ value of −0.133‰. The limited data on individual chondrules from Hamlet, an LL4-brecciated chondrite (*33*), show a very wide $\delta^{41}K$ range, with the most chondrules having lighter $\delta^{41}K$ than the bulk CI chondrites. This result is inconsistent with the fractional evaporative loss of K assumed by (*11*) but is in line with the observed addition of SiO_2 to crystallizing chondrule melts from the ambient gas (*34*–*36*). Because no reliable $\delta^{41}K$ value for chondrules is currently available, we approximate it by the $\delta^{41}K$ value of −0.692‰ from the bulk ordinary chondrites, which are known to contain up to 80 volume % chondrules (*37*). The $\delta^{41}K$ value of 0.249‰ for CAIs is calculated on the basis of the assumption that all ^{41}K is the product of ^{41}Ca decay (section S6.1), and the $\varepsilon^{64}Ni$ and $\varepsilon^{54}Cr$ values are from (*13*, *38*). The results of a three-component mixing are shown in Fig. 2. Because of the large positive anomalies of $\varepsilon^{64}Ni$ and $\varepsilon^{54}Cr$ in CAIs, the calculated mixing region is enriched in these nuclides and shifts away from the observed arrays, regardless of the $\delta^{41}K$ values in CAIs (Fig. 2 and fig. S8). Hence, our data cannot be explained by the mixing of major chondrite components.

The most likely interpretation for the correlations of $\delta^{41}K$ with $\varepsilon^{64}Ni$ and $\varepsilon^{54}Cr$ in bulk chondrites is presolar anomalies. As ^{41}Ca could also be partially produced by s-processes, the ^{41}K anomalies could arise from a combination of s-processes in other stars and a type II supernova explosion (consistent with ^{64}Ni). There is, however, not much evidence, so far, supporting an s-process origin, and our data thus preferentially suggest the type II supernova as the main source of presolar ^{41}K heterogeneity.

Implications for an isotopically heterogenous molecular cloud

Out of many scenarios regarding the formation of an isotopically heterogeneous protoplanetary disk, three are illustrated in Fig. 3. The first scenario assumes that isotopically homogeneous materials infalling from the molecular cloud experienced nebula-wide thermal processing, resulting in the formation of an isotopically heterogeneous inner disk depleted in MVEs (Fig. 3A). The partial evaporation of thermally unstable phases would fractionate nuclides of different origins to the same degree (e.g., ^{46}Ti and ^{50}Ti) (*39*). If so, the isotopic composition of an element should correlate with its MVE depletion, which is not observed for K (Fig. 1). We thus rule out this model.

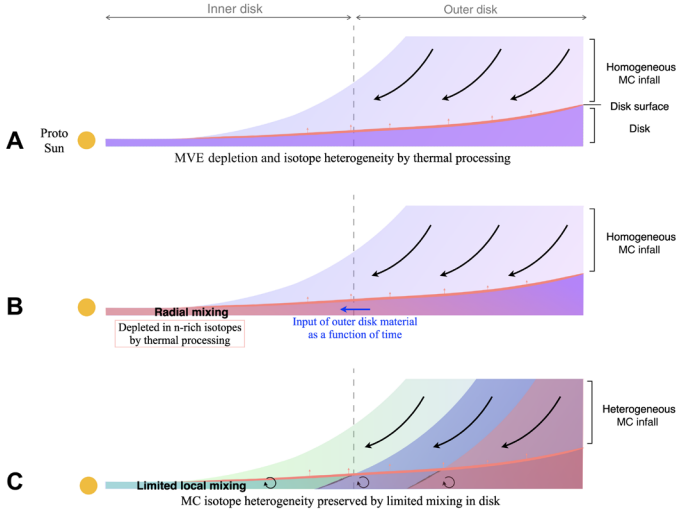

Fig. 3. Models explaining the observed isotopic heterogeneity and MVE depletions in the solar protoplanetary disk. (**A**) A nebular thermal processing of infalling, isotopically homogeneous material from the molecular cloud results in both isotopic heterogeneity (for $\varepsilon^{46}Ti$ and $\varepsilon^{50}Ti$) and variable depletions in MVEs in the disk (*39*). An expected correlation between isotope compositions and depletion of MVEs is not observed for K, ruling out this model. (**B**) Isotopic heterogeneity (for $\mu^{48}Ca$ and others) in the inner disk (depleted in n-rich isotopes) results from thermal processing of a homogeneous molecular cloud material. The inner disk gradually mixes with materials from the outer disk, making the isotopic composition of solid bodies in the inner solar system a function of time (increasing n-rich isotopes with time) (*16*). This would produce correlations among isotope compositions, MVE depletions, and sizes of planetary bodies in the inner solar system, which is not observed for K, ruling out this model too. (**C**) Isotopic heterogeneity inherited from an isotopically heterogeneous molecular cloud. Thermal processing in the disk produces the MVE depletions in the solid objects of the inner disk. No correlation between isotope compositions and MVE depletions is expected as long as mixing in the disk occurs on a local scale only, but the correlation between MVEs ($\delta^{41}K$) and other n-rich refractory nuclides ($\varepsilon^{64}Ni$, $\varepsilon^{54}Cr$) can be preserved. This is the model favored by our K isotope data.

In the second scenario (Fig. 3B), the degree of heterogeneity is time-dependent and reflects mixing between isotopically different materials from the inner and outer disk. Like in the first scenario, the protosolar disk forms from a homogeneous molecular cloud, but only the inner disk becomes depleted in neutron-rich isotopes during thermal processing. As the inner disk gradually mixes with the outer disk, the degree of isotopic heterogeneity changes with time. A special case of this scenario (*16*) predicts that larger, later-formed bodies like Earth would have heavier $\mu^{48}Ca$ than smaller, earlier-formed ones such as Mars and Vesta due to continuous admixing of isotopically heavier materials from the outer disk (i.e., carbonaceous chondrites). However, this case cannot explain the fact that Earth has lighter $\delta^{41}K$ than Mars. The lack of correlation between K depletion and $\delta^{41}K$ rules out thermal processing as the main cause for the inner-outer isotopic differences.

In the third scenario (Fig. 3C), isotopic heterogeneity in the protosolar disk was inherited from an isotopically heterogeneous molecular cloud. If so, the isotopic heterogeneity of both moderately volatile (^{41}K) and refractory (^{54}Cr and ^{64}Ni) nuclides preserved in meteorites can only be explained by a limited mixing of nucleosynthetic materials. The depletion in MVEs, caused by thermal processing, does not need to correlate with the isotopic composition as long as mixing in the disk occurs only on a local scale. It also implies that the feeding zones of planetesimals and planets are relatively narrow and do not mix with one another. The correlations between $\delta^{41}K$ and other neutron-rich refractory nuclide ($\varepsilon^{64}Ni$, $\varepsilon^{54}Cr$) anomalies can be preserved in this scenario. Thus, such a model is favored by our K data.

The survival of K isotopic heterogeneity implies a limited mixing among formation regions of the various planetary and chondrite parent bodies. Perhaps, any gaps in the protoplanetary disk [e.g., from early formation of planets (*40*–*42*)] can further segregate the presolar (pre-CAI formation) isotopically distinct reservoirs and serve as barriers against radial mixing. Such local isotopic heterogeneity can survive through later disk-wide disturbances [e.g., Grand Tack (*43*)] and would be preserved in the compositionally diverse asteroid belt where the most primitive meteorites might have come from (*44*). The isotopic anomalies, now, observed for both refractory and moderately volatile elements in primitive meteorites are inherited from the heterogeneous protosolar molecular cloud, which is likely associated with type II supernova injection before the solar system formed.

MATERIALS AND METHODS

We studied 15 ordinary (H, L, and LL), 11 carbonaceous (CI, CM, CV, CO, and CK), and 4 enstatite chondrites (EL and EH) of different petrologic types, both finds and falls, and 12 samples of differentiated planetary bodies, including 3 Martian meteorites, 4 eucrites, and 3 terrestrial samples. Whole-rock powders of four ordinary chondrites (Peace River-1, Bruderheim, Guareña, and Grady) were prepared by crushing and powdering >50 g of each meteorite. An additional 0.12-g powder aliquot of Peace River from a different source (Peace River-2 prepared from >5 g) was also analyzed to compare with a larger sample to test the sample representativeness of ordinary chondrites. Samples of other chondrites were prepared from >2 g rocks, which is sufficient to represent the bulk composition, with very few exceptions of carbonaceous chondrites. Samples weighing <5 g were crushed gently using high-purity aluminum oxide mortars and pestles to minimize possible metal contamination.

Samples of some meteorites were obtained from multiple sources to test homogeneity of these meteorites by repeated measurements; they are distinguished by Arabic numerals (Allende-1, Allende-2, etc.). In addition, we have tested the homogeneity of the sample powder by dissolving multiple aliquots of many samples. The separately dissolved aliquots of the same powdered sample have also passed through different columns to test the reproducibility of our column processing; such aliquots are marked by characters a and b (Allende-1-a, Allende-1-b, etc.) in Table 1.

Acid dissolution and chemical purification of potassium

Aliquots (50 to 150 mg) of the whole-rock powders were dissolved in multiple steps using mixtures of HF, HCl, and HNO_3. Samples were heated to 210°C in the CEM MARS 6 microwave digestion system repeatedly. After complete digestion, aliquots were redissolved in 0.5 N HNO_3 for K ion exchange column chemistry. The solutions were loaded on the 13-ml Bio-Rad AG50W-X8 cation-exchange resin (100 to 200 mesh) chromatography columns and processed with our established procedure (*18*), except less sample was loaded (~10 mg of whole rock). Solutions were passed through the columns twice to purify the K-cuts (>99% yield) and redissolved in dilute HNO_3 (~0.32 N) for ICP-MS analysis.

Mass spectrometry

The K isotopes were measured at Harvard University with the multicollector ICP-MS Nu Sapphire (serial no. SP001). We used the low-energy ion path and a hexapole collision cell to eliminate mass interferences from Ar-bearing ions such as ArH^+, Ar^+, and ArO^+. Solutions containing ~250 ppb (parts per billion) of K yield ~4 nA ^{39}K signal. Samples and standard were matched for ^{39}K intensity within 1%. A single analytical sample-standard bracketing run (about five repeats) consumes ~4 ml of the solution, equivalent to ~1 μg of K. We reported the measured K isotope values relative to our laboratory standard Merck Suprapur KNO_3 of 99.995% purity.

Because K analytical solutions could be contaminated with small amounts of Ca, we also measured mass 40 (for Ca) to monitor the possible formation of $^{40}CaH^+$ (mass 41 interferes with ^{41}K) in both analytical samples and standards. The contribution of $^{40}CaH^+$ to the mass 41 peak was calculated from the analysis of K standard solution spiked with Ca. The $\delta^{41}K$ values of all samples of a particular run were corrected for $^{40}CaH^+$ interference, typically less than 0.02‰. In addition, we monitored the quality of each analytical run by analyzing an extra standard solution with up to 20% concentration mismatch. Runs were considered acceptable only when the $\delta^{41}K$ difference between the "normal" and "mismatching" standard is less than 0.05‰ (an example is shown in fig. S1).

Accuracy and analytical uncertainties

High-precision isotope ratio measurements require repeated measurements to evaluate the uncertainty of a sample's mean value. The uncertainty was calculated and reported as doubled SE of the mean ($2\sigma_{SE}$). Error estimates need to be verified by comparing external reproducibility and internal uncertainty. Therefore, we have taken into account (i) within-run uncertainties, (ii) instrument day-to-day variability, and (iii) column chemistry and dissolution uncertainties. The first quantity is the internal uncertainty, while the second and third quantities are defined here as external reproducibility.

The within-run uncertainty is the calculated SE of a sample that was repeatedly measured within an analytical run, given by

$$2 \cdot \sigma_{SE} = 2 \cdot \frac{\sigma_{SD}}{\sqrt{n}}$$

where n is the bracketing repeats for a sample within a run (typically $n = 5$). The SD could be estimated by the self-bracketing on a standard within an analytical run (typically 2SD = 65 ppm). The internal uncertainty (2SE) was, thus, calculated as 30 ppm for a sample (fig. S2A). Uncertainties reported in Table 1 were replaced with 30 ppm if less than that value.

The external reproducibility takes into account the instrumental day-to-day variability and uncertainties of column processing and sample dissolution. The instrumental day-to-day variability was estimated by measuring one aliquot repeatedly on different days. We calculated the variations (2SD) of $\delta^{41}K$ values of a single aliquot, BHVO-2, which was measured for 9 days, to be 27 ppm. We reported this as our external reproducibility for a single measurement (fig. S2B). The consistency between internal (within-run) uncertainty (30 ppm) and external reproducibility (27 ppm) implies that there is no additional variability added to the data.

Figure S2C shows that the uncertainties of column chemistry and dissolution processes are negligible, even if the uncertainties from dissolution processes for meteorites may be larger than typical terrestrial samples due to materials (SiC, graphite, etc.) that are hard to dissolve. We compare the mean $\delta^{41}K$ values for two aliquots (a and b) from the same samples that were dissolved independently and analyzed on multiple days.

Calculating the group mean (Table 1)

The group mean and the corresponding 2SE are calculated on the basis of different meteorites. That is to say, if a meteorite was analyzed more than once, we first calculated the mean of these two or more analyses and then considered the calculated value as a single data point for the calculation of the group mean.

Most of the samples in this study were acquired from different sources, and some of them were dissolved and analyzed more than once. For instance, Allende was obtained from two different sources (Allende-1 and Allende-2), and Allende-1 was dissolved twice independently. The CV group mean should, however, consider Allende and Vigarano meteorites equally. We first calculate the mean $\delta^{41}K$ for Allende by averaging [mean (Allende-1a, Allende-1b), Allende-2]. Then, we calculate the mean for Vigarano-1 from averaging Vigarano-1a and Vigarano-1b. Last, the group mean for CV chondrites is the mean value of Allende (both Allende-1 and Allende-2) and Vigarano-1, which is −0.184.

SUPPLEMENTARY MATERIALS

Supplementary material for this article is available at http://advances.sciencemag.org/cgi/content/full/6/41/eabd0511/DC1

REFERENCES AND NOTES

1. E. Anders, N. Grevesse, Abundances of the elements: Meteoritic and solar. *Geochim. Cosmochim. Acta* **53**, 197–214 (1989).
2. M. Humayun, R. N. Clayton, Potassium isotope cosmochemistry: Genetic implications of volatile element depletion. *Geochim. Cosmochim. Acta* **59**, 2131–2148 (1995).
3. P. Cassen, Models for the fractionation of moderately volatile elements in the solar nebula. *Meteorit. Planet. Sci.* **31**, 793–806 (1996).
4. A. N. Halliday, D. Porcelli, In search of lost planets—The paleocosmochemistry of the inner solar system. *Earth Planet. Sci. Lett.* **192**, 545–559 (2001).
5. W. Kutschera, I. Ahmad, M. Paul, Half-life determination of ^{41}Ca and some other radioisotopes. *Radiocarbon.* **34**, 436–446 (1992).
6. F. M. McCubbin, M. A. Riner, K. E. V. Kaaden, L. K. Burkemper, Is Mercury a volatile-rich planet? *Geophys. Res. Lett.* **39**, L09202 (2012).

7. K. Wang, S. B. Jacobsen, Potassium isotopic evidence for a high-energy giant impact origin of the Moon. *Nature* **538**, 487–490 (2016).
8. C. Zhao, K. Lodders, H. Bloom, H. Chen, Z. Tian, P. Koefoed, M. K. Pető, K. Wang, Potassium isotopic compositions of enstatite meteorites. *Meteorit. Planet. Sci.* **55**, 1404–1417 (2020).
9. Z. Tian, H. Chen, B. Fegley Jr., K. Lodders, J.-A. Barrat, J. M. D. Day, K. Wang, Potassium isotopic compositions of howardite-eucrite-diogenite meteorites. *Geochim. Cosmochim. Acta* **266**, 611–632 (2019).
10. Y. Ku, S. B. Jacobsen, Potassium isotope variations in chondrites. *Lunar. Planet. Sci. Conf.* **50**, 1675 (2019).
11. H. Bloom, K. Lodders, H. Chen, C. Zhao, Z. Tian, P. Koefoed, M. K. Pető, Y. Jiang, K. Wang, Potassium isotope compositions of carbonaceous and ordinary chondrites: Implications on the origin of volatile depletion in the early solar system. *Geochim. Cosmochim. Acta* **277**, 111–131 (2020).
12. B. S. Meyer, D. D. Clayton, Short-lived radioactivities and the birth of the sun. *Space Sci. Rev.* **92**, 133–152 (2000).
13. A. Trinquier, J.-L. Birck, C. J. Allegre, Widespread ^{54}Cr heterogeneity in the inner solar system. *Astrophys. J.* **655**, 1179–1185 (2007).
14. L. Qin, C. M. O'D. Alexander, R. W. Carlson, M. F. Horan, T. Yokoyama, Contributors to chromium isotope variation of meteorites. *Geochim. Cosmochim. Acta* **74**, 1122–1145 (2010).
15. R. C. J. Steele, C. D. Coath, M. Regelous, S. Russell, T. Elliott, Neutron-poor nickel isotope anomalies in meteorites. *Astrophys. J.* **758**, 59 (2012).
16. M. Schiller, M. Bizzarro, V. A. Fernandes, Isotopic evolution of the protoplanetary disk and the building blocks of Earth and the Moon. *Nature* **555**, 507–510 (2018).
17. N. Dauphas, The isotopic nature of the Earth's accreting material through time. *Nature* **541**, 521–524 (2017).
18. K. Wang, S. B. Jacobsen, An estimate of the Bulk Silicate Earth potassium isotopic composition based on MC-ICPMS measurements of basalts. *Geochim. Cosmochim. Acta* **178**, 223–232 (2016).
19. F. M. Richter, R. A. Mendybaev, J. N. Christensen, D. Ebel, A. Gaffney, Laboratory experiments bearing on the origin and evolution of olivine-rich chondrules. *Meteorit. Planet. Sci.* **46**, 1152–1178 (2011).
20. K. Lodders, Solar system abundances and condensation temperatures of the elements. *Astrophys. J.* **591**, 1220–1247 (2003).
21. F. Moynier, P. Beck, F. Jourdan, Q.-Z. Yin, U. Reimold, C. Koeberl, Isotopic fractionation of zinc in tektites. *Earth Planet. Sci. Lett.* **277**, 482–489 (2009).
22. F. Moynier, P. Beck, Q.-Z. Yin, T. Ferroir, J.-A. Barrat, R. Paniello, P. Telouk, P. Gillet, Volatilization induced by impacts recorded in Zn isotope composition of ureilites. *Chem. Geol.* **276**, 374–379 (2010).
23. F. Moynier, C. Koeberl, P. Beck, F. Jourdan, P. Telouk, Isotopic fractionation of Cu in tektites. *Geochim. Cosmochim. Acta* **74**, 799–807 (2010).
24. Y. Jiang, H. Chen, B. Fegley Jr., K. Lodders, W. Hsu, S. B. Jacobsen, K. Wang, Implications of K, Cu and Zn isotopes for the formation of tektites. *Geochim. Cosmochim. Acta* **259**, 170–187 (2019).
25. B. J. Wood, M. J. Walter, J. Wade, Accretion of the Earth and segregation of its core. *Nature* **441**, 825–833 (2006).
26. J. N. Goswami, Short-lived nuclides in the early solar system. *Proc. Indian Acad. Sci. Earth Planet. Sci.* **107**, 401–411 (1998).
27. M.-C. Liu, M. Chaussidon, G. Srinivasan, K. D. McKeegan, A lower initial abundance of short-lived ^{41}Ca in the early solar system and its implications for solar system formation. *Astrophys. J.* **761**, 137 (2012).
28. D. Clayton, *Handbook of Isotopes in the Cosmos: Hydrogen to Gallium* (Cambridge Univ. Press, 2003).
29. F. X. Timmes, S. E. Woosley, D. H. Hartmann, R. D. Hoffman, T. A. Weaver, F. Matteucci, ^{26}Al and ^{60}Fe from supernova explosions. *Astrophys. J.* **449**, 204 (1995).
30. N. Prantzos, C. Doom, M. Arnould, C. de Loore, Nucleosynthesis and evolution of massive stars with mass loss and overshooting. *Astrophys. J.* **304**, 695–712 (1986).
31. M. Lugaro, A. Heger, D. Osrin, S. Goriely, K. Zuber, A. I. Karakas, B. K. Gibson, C. L. Doherty, J. C. Lattanzio, U. Ott, Stellar origin of the ^{182}Hf cosmochronometer and the presolar history of solar system matter. *Science* **345**, 650–653 (2014).
32. C. M. O'D. Alexander, Quantitative models for the elemental and isotopic fractionations in chondrites: The carbonaceous chondrites. *Geochim. Cosmochim. Acta* **254**, 277–309 (2019).
33. P. Koefoed, O. Pravdivtseva, H. Chen, C. Gerritzen, K. Wang, K Isotope systematics of individual chondrules from the LL4 chondrite Hamlet. *Lunar Planet. Sci. Conf.* **50**, 1672 (2019).
34. A. N. Krot, G. Libourel, C. A. Goodrich, M. I. Petaev, Silica-rich igneous rims around magnesian chondrules in CR carbonaceous chondrites: Evidence for condensation origin from fractionated nebular gas. *Meteorit. Planet. Sci.* **39**, 1931–1955 (2004).
35. M. Chaussidon, G. Libourel, A. N. Krot, Oxygen isotopic constraints on the origin of magnesian chondrules and on the gaseous reservoirs in the early Solar System. *Geochim. Cosmochim. Acta* **72**, 1924–1938 (2008).
36. G. Libourel, M. Portail, Chondrules as direct thermochemical sensors of solar protoplanetary disk gas. *Sci. Adv.* **4**, eaar3321 (2018).
37. E. R. D. Scott, A. N. Krot, Chondrites and their components. *Treatise Geochem.* **1**, 711 (2003).
38. J. L. Birck, G. W. Lugmair, Nickel and chromium isotopes in Allende inclusions. *Earth Planet. Sci. Lett.* **90**, 131–143 (1988).
39. A. Trinquier, T. Elliott, D. Ulfbeck, C. Coath, A. N. Krot, M. Bizzarro, Origin of nucleosynthetic isotope heterogeneity in the solar protoplanetary disk. *Science* **324**, 374–376 (2009).
40. T. S. Kruijer, C. Burkhardt, G. Budde, T. Kleine, Age of Jupiter inferred from the distinct genetics and formation times of meteorites. *Proc. Natl. Acad. Sci. U.S.A.* **114**, 6712–6716 (2017).
41. C. Pinte, D. J. Price, F. Ménard, G. Duchêne, W. R. F. Dent, T. Hill, I. de Gregorio-Monsalvo, A. Hales, D. Mentiplay, Kinematic evidence for an embedded protoplanet in a circumstellar disk. *Astrophys. J.* **860**, L13 (2018).
42. R. Teague, J. Bae, E. A. Bergin, T. Birnstiel, D. Foreman-Mackey, A kinematical detection of two embedded Jupiter-mass planets in HD 163296. *Astrophys. J. Lett.* **860**, L12 (2018).
43. K. J. Walsh, A. Morbidelli, S. N. Raymond, D. P. O'Brien, A. M. Mandell, A low mass for Mars from Jupiter's early gas-driven migration. *Nature* **475**, 206–209 (2011).
44. F. E. DeMeo, B. Carry, Solar System evolution from compositional mapping of the asteroid belt. *Nature* **505**, 629–634 (2014).
45. C. M. O'D. Alexander, Quantitative models for the elemental and isotopic fractionations in the chondrites: The non-carbonaceous chondrites. *Geochim. Cosmochim. Acta* **254**, 246–276 (2019).
46. G. J. Taylor, The bulk composition of Mars. *Geochemistry* **73**, 401–420 (2013).
47. W. F. McDonough, Compositional model for the Earth's core. *Treatise Geochem.* **2**, 568 (2003).
48. H. Chen, Z. Tian, B. Tuller-Ross, R. L. Korotev, K. Wang, High-precision potassium isotopic analysis by MC-ICP-MS: An inter-laboratory comparison and refined K atomic weight. *J. Anal. At. Spectrom* **34**, 160–171 (2019).
49. F.-Z. Teng, N. Dauphas, J. M. Watkins, Non-traditional stable isotopes: Retrospective and prospective. *Rev. Mineral. Geochem.* **82**, 1–26 (2017).
50. T. B. Coplen, Guidelines and recommended terms for expression of stable-isotope-ratio and gas-ratio measurement results. *Rapid Commun. Mass Spectrom.* **25**, 2538–2560 (2011).
51. Y. Li, W. Wang, Z. Wu, S. Huang, First-principles investigation of equilibrium K isotope fractionation among K-bearing minerals. *Geochim. Cosmochim. Acta* **264**, 30–42 (2019).
52. S. P. Verma, Seawater alteration effects on ^{87}Sr/^{86}Sr, K, Rb, Cs, Ba and Sr in oceanic igneous rocks. *Chem. Geol.* **34**, 81–89 (1981).
53. T. Kuwatani, K. Yoshida, K. Ueki, R. Oyanagi, M. Uno, S. Akaho, Sparse isocon analysis: A data-driven approach for material transfer estimation. *Chem. Geol.* **532**, 119345 (2020).
54. R. Ramaty, B. Kozlovsky, R. E. Lingenfelter, Light isotopes, extinct radioisotopes, and gamma-ray lines from low-energy cosmic-ray interactions. *Astrophys. J.* **456**, 525 (1996).
55. T. Lee, F. H. Shu, H. Shang, A. E. Glassgold, K. E. Rehm, Protostellar cosmic rays and extinct radioactivities in meteorites. *Astrophys. J.* **506**, 898–912 (1998).
56. M. Gounelle, F. H. Shu, H. Shang, A. E. Glassgold, K. E. Rehm, T. Lee, Extinct radioactivities and protosolar cosmic rays: Self-shielding and light elements. *Astrophys. J.* **548**, 1051–1070 (2001).
57. J. Bollard, J. N. Connelly, M. J. Whitehouse, E. A. Pringle, L. Bonal, J. K. Jørgensen, Å. Nordlund, F. Moynier, M. Bizzarro, Early formation of planetary building blocks inferred from Pb isotopic ages of chondrules. *Sci. Adv.* **3**, e1700407 (2017).
58. P. J. Sylvester, S. B. Simon, L. Grossman, Refractory inclusions from the Leoville, Efremovka, and Vigarano c3v chondrites: Major element differences between types A and B, and extraordinary refractory siderophile element compositions. *Geochim. Cosmochim. Acta* **57**, 3763–3784 (1993).
59. R. L. Rudnick, S. Gao, Composition of the continental crust. *Treatise Geochem.* **3**, 659 (2003).
60. Y. Hu, X.-Y. Chen, Y.-K. Xu, F.-Z. Teng, High-precision analysis of potassium isotopes by HR-MC-ICPMS. *Chem. Geol.* **493**, 100–108 (2018).
61. J. M. Luck, D. B. Othman, F. Albarède, Zn and Cu isotopic variations in chondrites and iron meteorites: Early solar nebula reservoirs and parent-body processes. *Geochim. Cosmochim. Acta* **69**, 5351–5363 (2005).
62. J. M. Luck, D. B. Othman, J. A. Barrat, F. Albarède, Coupled ^{63}Cu and ^{16}O excesses in chondrites. *Geochim. Cosmochim. Acta* **67**, 143–151 (2003).
63. M. Regelous, T. Elliott, C. D. Coath, Nickel isotope heterogeneity in the early Solar System. *Earth Planet. Sci. Lett.* **272**, 330–338 (2008).
64. H. Tang, N. Dauphas, Abundance, distribution, and origin of ^{60}Fe in the solar protoplanetary disk. *Earth Planet. Sci. Lett.* **359–360**, 248–263 (2012).
65. H. Tang, N. Dauphas, ^{60}Fe–^{60}Ni chronology of core formation in Mars. *Earth Planet. Sci. Lett.* **390**, 264–274 (2014).

66. N. Dauphas, D. L. Cook, A. Sacarabany, C. Fröhlich, A. M. Davis, M. Wadhwa, A. Pourmand, T. Rauscher, R. Gallino, Iron 60 evidence for early injection and efficient mixing of stellar debris in the protosolar nebula. *Astrophys. J.* **686**, 560–569 (2008).
67. A. Shukolyukov, G. W. Lugmair, Manganese–chromium isotope systematics of carbonaceous chondrites. *Earth Planet. Sci. Lett.* **250**, 200–213 (2006).
68. M. Schiller, E. V. Kooten, J. C. Holst, M. B. Olsen, M. Bizzarro, Precise measurement of chromium isotopes by MC-ICPMS. *J. Anal. At. Spectrom* **29**, 1406–1416 (2014).
69. K. K. Larsen, A. Trinquier, C. Paton, M. Schiller, D. Wielandt, M. A. Ivanova, J. N. Connelly, Å. Nordlund, A. N. Krot, M. Bizzarro, Evidence for magnesium isotope heterogeneity in the solar protoplanetary disk. *Astrophys. J. Lett.* **735**, L37 (2011).
70. C. Göpel, J.-L. Birck, A. Galy, J.-A. Barrat, B. Zanda, Mn–Cr systematics in primitive meteorites: Insights from mineral separation and partial dissolution. *Geochim. Cosmochim. Acta* **156**, 1–24 (2015).
71. M. Schiller, C. Paton, M. Bizzarro, Evidence for nucleosynthetic enrichment of the protosolar molecular cloud core by multiple supernova events. *Geochim. Cosmochim. Acta* **149**, 88–102 (2015).
72. N. Dauphas, J. H. Chen, J. Zhang, D. A. Papanastassiou, A. M. Davis, C. Travaglio, Calcium-48 isotopic anomalies in bulk chondrites and achondrites: Evidence for a uniform isotopic reservoir in the inner protoplanetary disk. *Earth Planet. Sci. Lett.* **407**, 96–108 (2014).
73. H.-W. Chen, T. Lee, D.-C. Lee, J. Jiun-San Shen, J.-C. Chen, ^{48}Ca heterogeneity in differentiated meteorites. *Astrophys. J. Lett.* **743**, L23 (2011).
74. J. Zhang, N. Dauphas, A. M. Davis, A. Pourmand, A new method for MC-ICPMS measurement of titanium isotopic composition: Identification of correlated isotope anomalies in meteorites. *J. Anal. At. Spectrom* **26**, 2197–2205 (2011).
75. J. Zhang, N. Dauphas, A. M. Davis, I. Leya, A. Fedkin, The proto-Earth as a significant source of lunar material. *Nat. Geosci.* **5**, 251–255 (2012).
76. R. Andreasen, M. Sharma, Solar nebula heterogeneity in p-process samarium and neodymium isotopes. *Science* **314**, 806–809 (2006).
77. A. Bouvier, J. D. Vervoort, P. J. Patchett, The Lu-Hf and Sm-Nd isotopic composition of CHUR: Constraints from unequilibrated chondrites and implications for the bulk composition of terrestrial planets. *Earth Planet. Sci. Lett.* **273**, 48–57 (2008).
78. A. Bouvier, M. Boyet, Primitive solar system materials and Earth share a common initial ^{142}Nd abundance. *Nature* **537**, 399–402 (2016).
79. M. Boyet, R. W. Carlson, ^{142}Nd evidence for early (>4.53 Ga) global differentiation of the silicate Earth. *Science* **309**, 576–581 (2005).
80. M. Boyet, R. W. Carlson, M. Horan, Old Sm–Nd ages for cumulate eucrites and redetermination of the solar system initial ^{146}Sm/^{144}Sm ratio. *Earth Planet. Sci. Lett.* **291**, 172–181 (2010).
81. C. Burkhardt, L. E. Borg, G. A. Brennecka, Q. R. Shollenberger, N. Dauphas, T. Kleine, A nucleosynthetic origin for the Earth's anomalous ^{142}Nd composition. *Nature* **537**, 394–398 (2016).
82. R. W. Carlson, M. Boyet, M. Horan, Chondrite barium, neodymium, and samarium isotopic heterogeneity and early Earth differentiation. *Science* **316**, 1175–1178 (2007).
83. A. Gannoun, M. Boyet, H. Rizo, A. E. Goresy, ^{146}Sm–^{142}Nd systematics measured in enstatite chondrites reveals a heterogeneous distribution of ^{142}Nd in the solar nebula. *Proc. Natl. Acad. Sci. U.S.A.* **108**, 7693–7697 (2011).
84. K. Rankenburg, A. D. Brandon, C. R. Neal, Neodymium isotope evidence for a chondritic composition of the Moon. *Science* **312**, 1369–1372 (2006).
85. P. Sprung, T. Kleine, E. E. Scherer, Isotopic evidence for chondritic Lu/Hf and Sm/Nd of the Moon. *Earth Planet. Sci. Lett.* **380**, 77–87 (2013).
86. C. Burkhardt, T. Kleine, F. Oberli, A. Pack, B. Bourdon, R. Wieler, Molybdenum isotope anomalies in meteorites: Constraints on solar nebula evolution and origin of the Earth. *Earth Planet. Sci. Lett.* **312**, 390–400 (2011).
87. C. Burkhardt, R. C. Hin, T. Kleine, B. Bourdon, Evidence for Mo isotope fractionation in the solar nebula and during planetary differentiation. *Earth Planet. Sci. Lett.* **391**, 201–211 (2014).
88. N. Dauphas, B. Marty, L. Reisberg, Molybdenum evidence for inherited planetary scale isotope heterogeneity of the protosolar nebula. *Astrophys. J.* **565**, 640–644 (2002).
89. N. Dauphas, B. Marty, L. Reisberg, Inference on terrestrial genesis from molybdenum isotope systematics. *Geophys. Res. Lett.* **29**, 1084 (2002).
90. N. Dauphas, B. Marty, L. Reisberg, Molybdenum nucleosynthetic dichotomy revealed in primitive meteorites. *Astrophys. J. Lett.* **569**, L139–L142 (2002).
91. E. M. M. E. Van Kooten, D. Wielandt, M. Schiller, K. Nagashima, A. Thomen, K. K. Larsen, M. B. Olsen, Å. Nordlund, A. N. Krot, M. Bizzarro, Isotopic evidence for primordial molecular cloud material in metal-rich carbonaceous chondrites. *Proc. Natl. Acad. Sci. U.S.A.* **113**, 2011–2016 (2016).
92. R. N. Clayton, T. K. Mayeda, The oxygen isotope record in Murchison and other carbonaceous chondrites. *Earth Planet. Sci. Lett.* **67**, 151–161 (1984).
93. R. N. Clayton, T. K. Mayeda, A. E. Rubin, Oxygen isotopic compositions of enstatite chondrites and aubrites. *J. Geophys. Res. Solid Earth.* **89**, C245–C249 (1984).
94. R. N. Clayton, T. K. Mayeda, K. Yanai, Oxygen isotopic compositions of some Yamato meteorites. *Natl. Inst. Polar Res. Mem.* **35**, 267 (1984).
95. R. N. Clayton, T. K. Mayeda, Oxygen isotopes in chondrules from enstatite chondrites: Possible identification of a major nebular reservoir. *Lunar Planet. Sci.* **16**, 142–143 (1985).
96. R. N. Clayton, T. K. Mayeda, T. Hiroi, M. Zolensky, M. E. Lipschutz, Oxygen isotopes in laboratory-heated CI and CM chondrites. *Meteorit. Planet. Sci.* **32**, A30 (1997).
97. R. N. Clayton, T. K. Mayeda, Oxygen isotope studies of carbonaceous chondrites. *Geochim. Cosmochim. Acta* **63**, 2089–2104 (1999).
98. R. N. Clayton, Isotopic variations in primitive meteorites. *Philos. Trans. R. Soc. Lond. Ser. Math. Phys. Sci.* **303**, 339–349 (1981).
99. R. N. Clayton, T. K. Mayeda, J. N. Goswami, E. J. Olsen, Oxygen isotope studies of ordinary chondrites. *Geochim. Cosmochim. Acta* **55**, 2317–2337 (1991).
100. R. N. Clayton, T. K. Mayeda, Oxygen isotope studies of achondrites. *Geochim. Cosmochim. Acta* **60**, 1999–2017 (1996).
101. R. N. Clayton, N. Onuma, T. K. Mayeda, A classification of meteorites based on oxygen isotopes. *Earth Planet. Sci. Lett.* **30**, 10–18 (1976).
102. M. W. Rowe, R. N. Clayton, T. K. Mayeda, Oxygen isotopes in separated components of CI and CM meteorites. *Geochim. Cosmochim. Acta* **58**, 5341–5347 (1994).
103. J. Halbout, M. Javoy, F. Robert, Oxygen isotopes in type 3 ordinary chondrites. *Lunar Planet. Sci.* **15**, 339–340 (1984).
104. J. Halbout, T. K. Mayeda, R. N. Clayton, Carbon isotopes and light element abundances in carbonaceous chondrites. *Earth Planet. Sci. Lett.* **80**, 1–18 (1986).
105. M. E. Zolensky, D. W. Mittlefehldt, M. E. Lipschutz, X. Xiao, R. N. Clayton, T. K. Mayeda, R. A. Barrett, M. M. Grady, The composition and mineralogy of EET 83334. *Meteoritics* **24**, 345 (1989).
106. M. E. Zolensky, D. W. Mittlefehldt, M. E. Lipschutz, M.-S. Wang, R. N. Clayton, T. K. Mayeda, M. M. Grady, C. Pillinger, B. David, CM chondrites exhibit the complete petrologic range from type 2 to 1. *Geochim. Cosmochim. Acta* **61**, 5099–5115 (1997).
107. M. M. Grady, A. L. Graham, D. J. Barber, D. Aylmer, G. Kurat, T. Ntaflos, U. Ott, H. Palme, B. Spettel, Yamato-82042: An unusual carbonaceous chondrite with CM affinities. *Mem. Natl. Inst. Polar Res. Spec. Issue*, 162–178 (1987).
108. T. K. Mayeda, R. N. Clayton, K. Yanai, Oxygen isotopic compositions of several Antartic meteorites. *Mem. Natl. Inst. Polar Res. Spec. Issue*, 144–150 (1987).
109. T. K. Mayeda, R. N. Clayton, C. A. Molini-Velsko, Oxygen and silicon isotopes in ALHA 81005. *Geophys. Res. Lett.* **10**, 799–800 (1983).
110. T. K. Mayeda, R. N. Clayton, A. Sodonis, Internal oxygen isotope variations in two unequilibrated chondrites. *Meteoritics* **24**, 301 (1989).
111. A. J. Brearley, E. R. D. Scott, K. Keil, R. N. Clayton, T. K. Mayeda, W. V. Boynton, D. H. Hill, Chemical, isotopic and mineralogical evidence for the origin of matrix in ordinary chondrites. *Geochim. Cosmochim. Acta* **53**, 2081–2093 (1989).
112. T. K. Mayeda, K. Yanai, R. N. Clayton, Another martian meteorite. *Lunar Planet. Sci. Conf.* **26**, 917 (1995).
113. D. Weber, R. N. Clayton, T. K. Mayeda, A. Bischoff, Unusual equilibrated carbonaceous chondrites and CO3 meteorites from the Sahara. *Lunar Planet. Sci.* **27**, 1395 (1996).
114. A. Bischoff, H. Palme, R. N. Clayton, T. K. Mayeda, T. Grund, B. Spettel, T. Geiger, M. Endreß, W. Beckerling, K. Metzler, New carbonaceous and type 3 ordinary chondrites from the Sahara Desert. *Meteoritics* **26**, 318 (1991).
115. S. B. Simon, L. Grossman, I. Casanova, S. Symes, P. Benoit, D. W. G. Sears, J. F. Wacker, Axtell, a new CV3 chondrite find from Texas. *Meteoritics* **30**, 42–46 (1995).
116. L. P. Keller, K. L. Thomas, R. N. Clayton, T. K. Mayeda, J. M. DeHart, D. S. McKay, Aqueous alteration of the Bali CV3 chondrite: Evidence from mineralogy, mineral chemistry, and oxygen isotopic compositions. *Geochim. Cosmochim. Acta* **58**, 5589–5598 (1994).
117. M. K. Weisberg, M. Prinz, R. N. Clayton, T. K. Mayeda, CV3 chondrites: Three subgroups, not two. *Meteorit. Planet. Sci.* **32**, A138–A139 (1997).
118. R. N. Clayton, T. K. Mayeda, Correlated oxygen and magnesium isotope anomalies in allende inclusions, I: Oxygen. *Geophys. Res. Lett.* **4**, 295–298 (1977).
119. J. C. Bridges, I. A. Franchi, M. M. Grady, A. S. Sexton, C. T. Pillinger, The δ^{18}O Composition of Feldspar and other minerals in Lafayette. *Meteorit. Planet. Sci.* **32**, A21 (1997).
120. J. C. Bridges, I. A. Franchi, A. S. Sexton, C. T. Pillinger, Mineralogical controls on the oxygen isotopic compositions of UOCs. *Geochim. Cosmochim. Acta* **63**, 945–951 (1999).
121. E. D. Young, S. S. Russell, Oxygen reservoirs in the early solar nebula inferred from an allende CAI. *Science* **282**, 452–455 (1998).
122. I. Jabeen, M. Kusakabe, K. Nagao, T. Nakamura, Oxygen isotope study of Tsukuba chondrite, some HED meteorites and Allende chondrules. *Antarct. Meteor. Res.* **11**, 122 (1998).
123. A. Ruzicka, D. A. Kring, D. H. Hill, W. V. Boynton, R. N. Clayton, T. K. Mayeda, Silica-rich orthopyroxenite in the Bovedy chondrite. *Meteoritics* **30**, 57–70 (1995).
124. N. Onuma, Y. Ikeda, T. K. Mayeda, R. N. Clayton, K. Yanai, Oxygen isotopic compositions of petrographically described inclusions from Antarctic unequilibrated ordinary-chondrites. *Mem. Nat. Inst. Polar Res.* **30**, 306–314 (1983).
125. J. N. Grossman, R. N. Clayton, T. K. Mayeda, Oxygen isotopes in the matrix of the semarkona (LL3.0) chondrite. *Meteoritics* **22**, 395 (1987).

126. S. I. Recca, E. R. D. Scott, K. Keil, R. N. Clayton, T. K. Mayeda, G. I. Huss, E. Jarosewich, K. S. Weeks, F. A. Hasan, D. W. G. Sears, R. Wieler, P. Signer, Ragland, an LI3.4 chondrite find from New Mexico. *Meteoritics* **21**, 217–229 (1986).
127. D. W. G. Sears, J. D. Batchelor, B. Mason, E. R. D. Scott, R. N. Clayton, T. K. Mayeda, South Australian type 3 chondrites. *Meteoritics* **25**, 407 (1990).
128. I. A. Franchi, T. Akagi, C. T. Pillinger, Laser fluorination of meteorites—Small sample analysis of $\delta^{17}O$ and $\delta^{18}O$. *Meteoritics* **27**, 222 (1992).
129. I. A. Franchi, I. P. Wright, A. S. Sexton, C. T. Pillinger, The oxygen-isotopic composition of Earth and Mars. *Meteorit. Planet. Sci.* **34**, 657–661 (1999).
130. C. S. Romanek, E. C. Perry, A. H. Treiman, R. A. Socki, J. H. Jones, E. K. Gibson Jr., Oxygen isotopic record of silicate alteration in the Shergotty–Nakhla–Chassigny meteorite Lafayette. *Meteorit. Planet. Sci.* **33**, 775–784 (1998).
131. E. D. Young, I. E. Kohl, P. H. Warren, D. C. Rubie, S. A. Jacobson, A. Morbidelli, Oxygen isotopic evidence for vigorous mixing during the Moon-forming giant impact. *Science* **351**, 493–496 (2016).

Acknowledgments: We thank three anonymous reviewers who provided helpful comments on the manuscript. We thank the Center for Meteorite Studies (ASU), the Harvard Museum of Natural History, the Museum national d'Histoire naturelle, the NASA Antarctic meteorite collection, J. Wood, J. Wasserburg, and U. Marvin for graciously providing most of the meteorites. We thank C. Langmuir for providing the East Pacific Ridge MORB sample used in this work. We also thank C. Parendo for experiment assistance, M. I. Petaev and M.-C. Liu for helpful discussions, and M. Petö for help in preparation of six meteorites. **Funding:** This work was supported by the NASA Emerging Worlds Program grant number 80NSSC20K0346. **Author contributions:** Y.K. and S.B.J. designed the research. Y.K. conducted the analytical work. Both authors participated in the interpretation of the data. Y.K. wrote the manuscript with input from S.B.J. **Competing interests:** The authors declare that they have no competing interests. **Data and materials availability:** All data needed to evaluate the conclusions in the paper are present in the paper and/or the Supplementary Materials. Additional data related to this paper may be requested from the authors.

Submitted 28 May 2020
Accepted 19 August 2020
Published 9 October 2020
10.1126/sciadv.abd0511

Citation: Y. Ku, S. B. Jacobsen, Potassium isotope anomalies in meteorites inherited from the protosolar molecular cloud. *Sci. Adv.* **6**, eabd0511 (2020).

Science Advances

Potassium isotope anomalies in meteorites inherited from the protosolar molecular cloud

Y. Ku and S. B. Jacobsen

Sci Adv **6** (41), eabd0511.
DOI: 10.1126/sciadv.abd0511

Science Advances (ISSN 2375-2548) is published by the American Association for the Advancement of Science, 1200 New York Avenue NW, Washington, DC 20005. The title *Science Advances* is a registered trademark of AAAS.